Effects of interactions, structure formation, and polydispersity on the dynamic magnetic susceptibility and magnetic relaxation of ferrofluids

Journal of Molecular Liquids 356 (2022) 119034

Contents lists available at ScienceDirect

Journal of Molecular Liquids

journal homepage: www.elsevier.com/locate/molliq

Effects of interactions, structure formation, and polydispersity on the dynamic magnetic susceptibility and magnetic relaxation of ferrofluids ☆

Alexey O. Ivanov [a], Philip J. Camp [b,*]

[a] Department of Theoretical and Mathematical Physics, Institute of Natural Sciences and Mathematics, Ural Federal University, 51 Lenin Avenue, Ekaterinburg 620000, Russia
[b] School of Chemistry, University of Edinburgh, David Brewster Road, Edinburgh EH9 3FJ, Scotland, United Kingdom

ARTICLE INFO

Article history:
Received 21 January 2022
Revised 24 March 2022
Accepted 26 March 2022
Available online 31 March 2022

Keywords:
Ferrofluids
Dynamic magnetic susceptibility
Fokker–Planck-Brown equation
Brownian dynamics simulations

ABSTRACT

Linear response theory relates the decay of equilibrium magnetisation fluctuations in a ferrofluid to the frequency-dependent response of the magnetisation to a weak ac external magnetic field. The characteristic relaxation times are strongly affected by interactions between the constituent particles. Similarly, the relaxation of an initially magnetised system towards equilibrium in zero field occurs on a range of timescales depending on the structure of the initial state, and the interactions between the particles. In this work, ferrofluids are modelled as colloidal suspensions of spherical particles carrying point dipole moments, and undergoing Brownian motion. Recent theoretical and simulation work on the relaxation and linear response of these model ferrofluids is reviewed, and the effects of interactions, structure formation, and polydispersity on the characteristic time scales are outlined. It is shown that: (i) in monodisperse ferrofluids, the timescale characterising the collective response to weak fields increases with increasing interaction strength and/or concentration; (ii) in monodisperse ferrofluids, the initial, short-time decay is independent of interaction strength, but the asymptotic relaxation time is the same as that characterising the collective response to weak fields; (iii) in the strong-interaction regime, the formation of self-assembled chains and rings introduces additional timescales that vary by orders of magnitude; and (iv) in polydisperse ferrofluids, the instantaneous magnetic relaxation time of each fraction varies in a complex way due to the role of interactions.

1. Introduction

Ferrofluids are colloidal suspensions of single-domain, ferromagnetic nanoparticles in a non-magnetic carrier liquid [1]. They are widely used in applications such as switchable optical media, sealants, heat conductors, separation media, gas-fluidised beds, and smart hydraulics. There is growing interest in applying ferrofluids as sensors [2,3], in nanoscale characterisation [4,5], for targeted drug delivery [6,7], and as heating media in magnetic hyperthermia treatments [8–10]. In this last example, the ferrofluid is exposed to an ac external magnetic field, and energy is dissipated as heat. The heating rate is proportional to the imaginary, or out-of-phase, component of the dynamic magnetic susceptibility $\chi(\omega) = \chi'(\omega) + i\chi''(\omega)$ [11–14]. $\chi(\omega)$ characterises the *linear* response of the magnetisation to a *weak* ac field [15,16]. The peak frequency in the imaginary part is controlled by the intrinsic rotation time of the magnetic nanoparticles [17,18], and the magnetic interactions between the particles. In general, stronger interactions lead to more collective reorientational motions of the particles, and hence an increase in the characteristic rotation time.

In other applications of ferrofluids, the optical and magnetic properties are controlled by strong, static external magnetic fields. In this case, the relaxation time of the magnetisation from a saturated state (in a strong field) to the demagnetised state (in zero field) is an important quantity, as it controls the ultimate switching rate [19–26]. (The reverse case is not considered here, although the magnetisation rate will in general be different from the relaxation rate.)

The topic of this contribution is the relationship between the time scales for the linear response, and the time scales for relaxation from an initially aligned state. In the first case, linear-response theory relates the frequency-dependent response to the decay of equilibrium fluctuations in the magnetisation; the key relationship is reviewed in Section 3. In the second case, the relaxation is measured by preparing the system in a strong aligning field – outwith the linear-response regime – and then switching off the

☆ Pálinkás 80 Festschrift.

* Corresponding author at: School of Chemistry, University of Edinburgh, David Brewster Road, Edinburgh EH9 3FJ, Scotland, United Kingdom.
E-mail address: philip.camp@ed.ac.uk (P.J. Camp).

https://doi.org/10.1016/j.molliq.2022.119034
0167-7322/

field. It is not obvious to what extent the same time scales appear in both processes, and this will be explored herein. The theoretical framework is based on Brownian dynamics, i.e., a particle's magnetic dipole moment is fixed within the body frame, and reorientation happens by particle rotation. The contribution from Néel relaxation will not be considered [1]. The Fokker–Planck-Brown equation for the Brownian rotation of a single particle [27–29] will be coupled with effective-field methods to describe the interparticle interactions; the so-called modified mean-field and modified-Weiss theories will be used, as these have been tested thoroughly against Brownian dynamics simulations, and shown to be reliable for moderately strong interactions [30,31].

The rest of this article is organised as follows. The basic ferrofluid properties, and essential elements of the theory (Fokker–Planck-Brown equation), are summarised in Section 2. In Section 3, the theoretical description of the frequency-dependent, linear response in monodisperse ferrofluids is outlined. The magnetic relaxation in monodisperse ferrofluids is described in Section 4, and compared and contrasted with the linear response. A brief description of the effects of strong interactions and clustering of monodisperse particles on the dynamic magnetic susceptibility and magnetic relaxation is given in Section 5. The extensions of these properties to polydisperse ferrofluids, with and without interactions, are considered in Section 6. Section 7 concludes the article.

2. Model and theoretical methods

The ferrofluid is modelled as a system of N particles in a volume V at temperature T. If particle j has hydrodynamic diameter σ_j and magnetic dipole moment $\boldsymbol{\mu}_j$, then the total volume fraction φ, effective dipolar coupling constant λ, and Langevin susceptibility $\chi_{\rm L}$ are given by

$$\varphi = \frac{\pi}{6V}\sum_{j=1}^{N}\sigma_j^3 = \frac{\pi\rho\langle\sigma^3\rangle}{6} \tag{1}$$

$$\lambda = \frac{\mu_0}{4\pi k_{\rm B}T}\frac{\sum_{j=1}^{N}\mu_j^2}{\sum_{j=1}^{N}\sigma_j^3} = \frac{\mu_0\langle\mu^2\rangle}{4\pi k_{\rm B}T\langle\sigma^3\rangle} \tag{2}$$

$$\chi_{\rm L} = \frac{\mu_0}{3Vk_{\rm B}T}\sum_{j=1}^{N}\mu_j^2 = \frac{4\pi}{3}\rho\langle\sigma^3\rangle\lambda = 8\varphi\lambda \tag{3}$$

where $\rho = N/V$ is the number concentration, μ_0 is the vacuum permeability, $k_{\rm B}$ is Boltzmann's constant, and $\langle\ldots\rangle$ denotes an average over the particle-size distribution. Note that there is no unique definition of the dipolar coupling constant in a polydisperse system; for instance, it could also be defined as being proportional to $\langle\mu^2/\sigma^3\rangle$. But the definition used here is convenient, because of the relationship in Eq. (3). The magnetic core diameter x is different from the hydrodynamic diameter σ, due to the presence of a demagnetised layer, and an adsorbed surfactant layer providing steric stabilisation. It is common to describe the particle size distribution with a probability density function $p(x)$. The dipole moment on a particle is proportional to the magnetic core volume, i.e., $\mu \propto x^3$. In the numerical examples discussed here, it will be assumed that $\sigma = x$, which makes things simple, but without losing any important information.

The Fokker–Planck-Brown (FPB) equation describing the Brownian rotational motion of particle 1 is [27–29]

$$2\tau_{\rm B}\frac{\partial W}{\partial t} = \frac{\partial}{\partial z}\left[(1-z^2)\left(\frac{\partial W}{\partial z} + \frac{W}{k_{\rm B}T}\frac{\partial U_1}{\partial z} + \frac{\rho}{k_{\rm B}T}\int\langle g_{12}\frac{\partial U_{12}}{dz}\rangle d\boldsymbol{r}_2\right)\right] \tag{4}$$

where t is the time, $\tau_{\rm B}$ is the Brownian rotation time, $W = W(z,t)$ is the one-particle orientational distribution function (ODF), $z = \cos\theta_1$ represents the orientation of the particle's dipole with respect to the laboratory Z axis, U_1 is the interaction energy between the particle and the external field, g_{12} is the pair distribution function, and U_{12} is the interaction energy between particles 1 and 2. For a particle in a liquid with viscosity η, the Brownian time is given by

$$\tau_{\rm B} = \frac{\pi\eta\sigma^3}{2k_{\rm B}T}. \tag{5}$$

The angled brackets $\langle\cdots\rangle$ in Eq. (4) denote an average over both the size and the orientation of particle 2. The interaction energy between the particle and an ac external field $\boldsymbol{H}(t)$ in the laboratory Z direction is

$$U_1 = -\mu_0\boldsymbol{\mu}_1\cdot\boldsymbol{H}(t) = -(\mu_0\mu_1 H_0 e^{-i\omega t})z \tag{6}$$

where to be clear, $z = \cos\theta_1$ refers to the *orientation* of the particle with respect to the laboratory Z axis. The interaction energy between two different particles is

$$U_{12} = \frac{\mu_0}{4\pi}\left[\frac{(\boldsymbol{\mu}_1\cdot\boldsymbol{\mu}_2)}{r^3} - \frac{3(\boldsymbol{\mu}_1\cdot\boldsymbol{r})(\boldsymbol{\mu}_2\cdot\boldsymbol{r})}{r^5}\right] \tag{7}$$

where $\boldsymbol{r}$ is the centre-centre separation vector, and $r = |\boldsymbol{r}|$. The FPB equation can be solved in two distinct ways, depending on the situation: (1) to study the dynamic magnetic susceptibility, the ac external field is considered to be weak, such that the Langevin parameter $\alpha = \mu_0\mu_1 H_0/k_{\rm B}T \ll 1$, and the periodic one-particle orientational distribution function determines the magnetic response of the system; and (2) to study the magnetic relaxation, the external field is set to zero, the initial condition corresponds to perfect alignment of all particles' dipole moments, and the time-dependent one-particle orientational distribution function determines the approach to equilibrium, meaning zero magnetisation. In both cases, the interaction term is determined approximately according to a mean-field approach, as detailed below.

3. Dynamic susceptibility of monodisperse ferrofluids

If the field strength is $H(t) = H_0 e^{-i\omega t}$, and the dynamic magnetic susceptibility is $\chi(\omega) = \chi'(\omega) + i\chi''(\omega)$, then the magnetisation is

$$M(t) = \chi(\omega)H(t) = M_0 e^{-i(\omega t-\delta)} \tag{8}$$

where $M_0\cos\delta = \chi' H_0, M_0\sin\delta = \chi'' H_0$, and the phase lag is $0 \leqslant \delta = \arctan(\chi''/\chi') \leqslant \pi/2$ (the magnetisation lags behind the field). The power loss is proportional to the imaginary part of the dynamic magnetic susceptibility, χ'' [11,32].

Linear response theory leads to an important relationship between $\chi(\omega)$ and the time correlation function $C(t)$ of equilibrium magnetisation fluctuations in zero field [33].

$$\frac{\chi(\omega)}{\chi(0)} = 1 + i\omega\int_0^\infty C(t)e^{i\omega t}dt \tag{9}$$

$C(t)$ is defined by

$$C(t) = \frac{\langle\boldsymbol{M}(t)\cdot\boldsymbol{M}(0)\rangle}{\langle\boldsymbol{M}(0)\cdot\boldsymbol{M}(0)\rangle} \tag{10}$$

and of course $\langle\boldsymbol{M}(t)\rangle = 0$. This provides a convenient route to calculating $\chi(\omega)$ from Brownian dynamics simulations, as has been demonstrated in recent work [30,34–36]. Such simulation results have been used to test the predictions of various theories that incorporate interactions, as outlined below.

In the ideal case – which corresponds to the original Debye theory [32,37] – the time correlation function is simply

$$C_{\rm D}(t) = e^{-t/\tau_{\rm B}} \tag{11}$$

and the real and imaginary parts of the dynamic magnetic susceptibility are then given by

$$\chi'_{\rm D}(\omega) = \frac{\chi_{\rm L}}{1+\omega^2\tau_{\rm B}^2} \tag{12a}$$

$$\chi''_{\rm D}(\omega) = \frac{\chi_{\rm L}\omega\tau_{\rm B}}{1+\omega^2\tau_{\rm B}^2} \tag{12b}$$

where the static susceptibility $\chi_{\rm D}(0)$ is equal to the Langevin value $\chi_{\rm L}$. Note that $\chi''_{\rm D}(\omega)$ shows a maximum at the frequency $\omega\tau_{\rm B}=1$, which provides a useful feature for measuring the effective relaxation time(s) in other situations.

There have been many attempts to include the effects of interactions [38–44]. The basic phenomenology is that interactions between particles lead to more collective motions, and since these are slower than single-particle motions, the peak frequency in $\chi''(\omega)$ decreases [45–47]. The approach taken here is to make approximations to the two-particle correlation function g_{12} in the FPB equation [Eq. (4)]. In the modified mean-field (MMF) theory, g_{12} is approximated by the function $W_1 W_2^{\rm D}\Theta_{12}$, where W_1 for particle 1 is to be determined, $W_2^{\rm D}$ is the ODF for particle 2 from the Debye theory, and Θ_{12} is the Heaviside step function that forbids two particles from overlapping with one another. The result for the dynamic magnetic susceptibility can be expressed entirely in terms of $\chi_{\rm D}(\omega)$ [48,49].

$$\chi'_{\rm MMF}(\omega) = \chi'_{\rm D}(\omega) + \frac{1}{3}\left\{\left[\chi'_{\rm D}(\omega)\right]^2 - \left[\chi''_{\rm D}(\omega)\right]^2\right\} \tag{13a}$$

$$\chi''_{\rm MMF}(\omega) = \chi''_{\rm D}(\omega)\left[1+\frac{2}{3}\chi'_{\rm D}(\omega)\right] \tag{13b}$$

Note that the static susceptibility is given by $\chi_{\rm MMF}(0) = \chi_{\rm L}(1+\chi_{\rm L}/3)$, which is the well-known result derived long ago [50–52]. These results have been tested against both experimental [48,49,53] and simulation data [34,54], and they are reliable as long as the Langevin parameter $\chi_{\rm L} \leqslant 1$.

In the Weiss theory [30], $g_{12} = W_1 W_2 \Theta_{12}$ and W_i is to be determined self-consistently. The final result for the dynamic magnetic susceptibility is

$$\chi_{\rm W} = \frac{\chi_{\rm D}(\omega)}{1-\frac{1}{3}\chi_{\rm D}(\omega)} \tag{14}$$

where again, everything is expressed in terms of the Debye functions. The problem with this expression is that the static susceptibility is predicted to diverge when $\chi_{\rm L}=3$, which does not occur in practice. A trick to remove the divergence and retain the MMF expression for the static susceptibility, is to multiply top and bottom by $(1+\chi_{\rm L}/3)$, and remove the bilinear term $\chi_{\rm L}\chi_{\rm D}(\omega)/9$. The resulting 'modified-Weiss' (MW) theory is therefore

$$\chi_{\rm MW}(\omega) = \frac{(1+\frac{1}{3}\chi_{\rm L})\chi_{\rm D}(\omega)}{1+\frac{1}{3}\chi_{\rm L}-\frac{1}{3}\chi_{\rm D}(\omega)} \tag{15}$$

from which the real and imaginary parts can be separated out easily. Comparisons with computer-simulation results show that the MW theory is marginally better than the MMF theory, and that the predictions are reliable for systems with $\chi_{\rm L} \leqslant 3$ [30].

4. Relaxation dynamics of monodisperse ferrofluids

The relaxation function $m(t)$ resembles $C(t)$, except that $\boldsymbol{M}(0) = N\mu\widehat{\boldsymbol{Z}}$ is the saturation magnetisation at $t=0$, when the strong aligning field in the Z direction is turned off.

$$m(t) = \frac{\overline{\boldsymbol{M}}(t)\cdot\boldsymbol{M}(0)}{\boldsymbol{M}(0)\cdot\boldsymbol{M}(0)} = \frac{\sum_{n=1}^{N}\overline{\boldsymbol{\mu}}_n(t)\cdot\widehat{\boldsymbol{Z}}}{N\mu} \tag{16}$$

The bar $\overline{\cdots}$ denotes an average over repeated realisations of the relaxation process. In the ideal case, meaning without interactions between the particles, the relaxation function is simply

$$m_{\rm id}(t) = e^{-t/\tau_{\rm B}}. \tag{17}$$

Hence, there is only one characteristic timescale, and $m(t)$ is identical to $C(t)$ in the Debye theory.

As with the dynamic magnetic susceptibility, interactions reduce the relaxation rate due to increased correlations between particles leading to collective motions [55–58]. Interactions can be included using approximations similar to those used in the calculation of the dynamic magnetic susceptibility. Within the MMF approach, the relaxation function is [31]

$$m_{\rm MMF}(t) = \left\{1+\frac{\chi_{\rm L}}{3}\left[\frac{t}{\tau_{\rm B}}+\frac{1}{3}\left(e^{-3t/\tau_{\rm B}}-1\right)\right]\right\}e^{-t/\tau_{\rm B}}. \tag{18}$$

This function has the unphysical feature of showing non-monotonic decay with large values of $\chi_{\rm L}$, but it is at least a leading-order approximation for the case of interacting particles. The MW expression – again with a trick to remove divergences – is more complicated, but it possesses entirely physical features [31].

$$m_{\rm MW}(t) = \exp\left\{-\frac{3t/\tau_{\rm B}+\ln\left[1+\chi_{\rm L}(1-e^{-3t/\tau_{\rm B}})/3\right]}{3+\chi_{\rm L}}\right\} \tag{19}$$

In this theory, the short-time decay is

$$m_{\rm MW}(t) \approx \exp\left(-\frac{t}{\tau_{\rm B}}\right) \tag{20}$$

while the asymptotic, long-time decay is

$$m_{\rm MW}(t) \sim \exp\left[-\frac{t}{(1+\chi_{\rm L}/3)\tau_{\rm B}}\right] \tag{21}$$

and this crossover has been verified using Brownian dynamics simulations [31].

To illustrate the difference between $C(t)$ and $m(t)$ in the presence of interactions, it is convenient to define the following function, which is analogous to the linear-response expression for the dynamic initial susceptibility.

$$K(\omega) = 1 + i\omega\int_0^\infty m(t)e^{i\omega t}dt \tag{22}$$

Comparing $K(\omega)$ with $\chi(\omega)/\chi(0)$ [*cf.* Eq. (9)] is easier than calculating $C(t)$ by the inverse Fourier transform of the corresponding $\chi(\omega)$. For the MMF theory, this gives $K(\omega) = K'(\omega) + iK''(\omega)$ with

$$K'_{\rm MMF}(\omega) = \frac{1}{1+s^2} - \frac{2\chi_{\rm L}}{3}\frac{s^2}{\left(1+s^2\right)^2} + \frac{\chi_{\rm L}}{9}\left(\frac{s^2}{1+s^2}-\frac{s^2}{16+s^2}\right) \tag{23a}$$

$$K''_{\rm MMF}(\omega) = \frac{s}{1+s^2} + \frac{\chi_{\rm L}}{3}\frac{\left(s-s^3\right)}{\left(1+s^2\right)^2} + \frac{\chi_{\rm L}}{9}\left(\frac{4s}{16+s^2}-\frac{s}{1+s^2}\right) \tag{23b}$$

where $s=\omega\tau_{\rm B}$. The Fourier transform of the MW expression [Eq. (19)] has to be done numerically.

$\chi(\omega)$ and $K(\omega)$ are compared in Fig. 1 for the specific case when $\chi_{\rm L}=1$. Fig. 1(a) and (b) show the results for the MMF theory, and Fig. 1(c) and (d) show the results for the MW theory. In each case, the corresponding Debye function $\chi_{\rm D}$ is shown, which represents the case of non-interacting particles. For both theories, and for both the real and imaginary parts, $K(\omega)$ is closer to $\chi(\omega)$ (with interactions) at low frequency, and closer to $\chi_{\rm D}(\omega)$ (no interactions) at high frequency. This represents the crossover in the relaxation function from the short-time behaviour with relaxation time

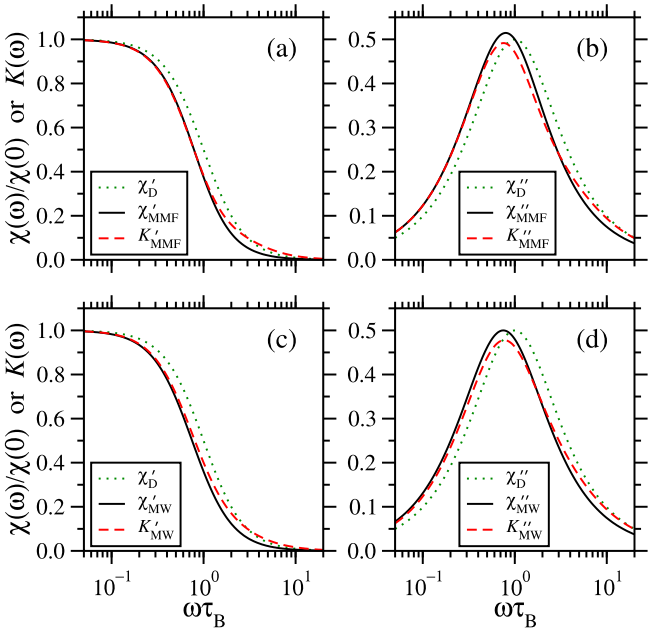

Fig. 1. A comparison of the spectra of $C(t)$ and $m(t)$ in the form of the dynamic initial susceptibility, being $\chi(\omega)/\chi(0)$ [Eq. (9)] and $K(\omega)$ [Eq. (22)], respectively. (a) and (b) show the real and imaginary parts from the MMF theory with $\chi_L = 1$. (c) and (d) show the real and imaginary parts from the MW theory with $\chi_L = 1$. In each case, the corresponding Debye function is shown for comparison, which corresponds to $\chi_L = 0$.

equal to τ_B, to the asymptotic, long-time behaviour with relaxation time equal to $(1 + \chi_L/3)\tau_B$. The general point is that the weak-field response cannot be inferred exactly from the relaxation function $m(t)$; it is properly related to the equilibrium time correlation function $C(t)$ through Eq. (9).

5. Effects of structure formation

It is well known that at low concentrations $\varphi \ll 0.1$, and with high dipolar coupling constant $\lambda > 4$, dipolar particles self-assemble to form chain-like and ring-like clusters [59,60]. The impact of these structures on the static magnetic susceptibility is that, increasing λ to about 6, the formation of chains increases $\chi(0)$, because of the strong orientational correlations between particles in a given chain. But above $\lambda \simeq 6$, the chains start to close up, forming rings with low net dipole moment, and hence $\chi(0)$ decreases [61].

A recent study on systems with $\varphi = 0.001$ and $1 \leqslant \lambda \leqslant 8$ has uncovered pronounced effects of clustering on the dynamic magnetic susceptibility as well [36]. Firstly, the formation of chains leads to an increase in the effective rotation time, and hence $\chi''(\omega)$ shows a low peak frequency, well below the single-particle frequency τ_B^{-1}. Secondly, as chains start to close up to form rings, a high-frequency feature appears in $\chi(\omega)$. This feature is associated with intracluster, single-particle reorientational motions, which can be well described with a simple mean-field theory; the corresponding frequency is at least an order of magnitude larger than the single-particle frequency. The reason why this feature is not observed in the chain regime is that the instantaneous magnetisation is dominated by the dipole moments of the chains, and the small modulations due to intracluster motions are drowned out. Since rings have low net dipole moments, it is possible to resolve the intracluster contributions to $\chi(\omega)$.

The effects of chain formation on magnetic relaxation have also been explored [31]. As noted in Section 4, the initial decay time is always equal to τ_B. But in the presence of chains, the asymptotic decay time far exceeds that predicted by theory, due to the reorientational relaxation of the chains themselves, and the exchange and reorientation of individual particles, all of which are slow processes, and are not captured in a simple theory.

6. Extensions to polydisperse ferrofluids

The extensions of some of these ideas to polydisperse ferrofluids are outlined here. Firstly, the susceptibility and relaxation in ideal polydisperse ferrofluids are summarised in Section 6.1. Then some initial results on the effects of interactions – within the MMF model – are presented in Section 6.2.

6.1. Susceptibility and relaxation in the ideal case

The time correlation function $C(t)$ in the case of Debye theory is given by

$$C_D(t) = \frac{\langle \mu^2 e^{-t/\tau_B} \rangle}{\langle \mu^2 \rangle} \tag{24}$$

where $\langle \cdots \rangle$ indicates an average over the particle-size distribution. The μ^2 weighting is important, and of course τ_B itself depends on the particle diameter through Eq. (5). An instantaneous relaxation time $\tau_{\rm eff}(t)$ can be defined, and its initial value can be evaluated.

$$\tau_{\rm eff}(t) = -\left(\frac{d \ln C_D}{dt}\right)^{-1} \tag{25a}$$

$$\tau_{\rm eff}(0) = \frac{\langle \mu^2 \rangle}{\langle \mu^2 \tau_B^{-1} \rangle} \tag{25b}$$

Note that if the hard-core diameter is the same as the magnetic-core diameter ($\sigma = x$), then $\mu^2 \propto \tau_B^2$, and hence $\tau_{\rm eff}(0) = \langle \tau_B^2 \rangle / \langle \tau_B \rangle$. Finally, the real and imaginary parts of the dynamic magnetic susceptibility are as follows.

$$\frac{\chi'_D(\omega)}{\chi(0)} = \frac{1}{\langle \mu^2 \rangle} \left\langle \frac{\mu^2}{1 + \omega^2 \tau_B^2} \right\rangle \tag{26a}$$

$$\frac{\chi''_D(\omega)}{\chi(0)} = \frac{1}{\langle \mu^2 \rangle} \left\langle \frac{\mu^2 \omega \tau_B}{1 + \omega^2 \tau_B^2} \right\rangle \tag{26b}$$

The equations for the magnetic relaxation function are very similar, except that the particle size dependent weighting is now proportional to μ, instead of μ^2.

$$m_{\rm id}(t) = \frac{\langle \mu e^{-t/\tau_B} \rangle}{\langle \mu \rangle} \tag{27}$$

An instantaneous relaxation time, and its initial value, can be defined just as before.

$$\tau_{\rm eff}(t) = -\left(\frac{d \ln m_{\rm id}}{dt}\right)^{-1} \tag{28a}$$

$$\tau_{\rm eff}(0) = \frac{\langle \mu \rangle}{\langle \mu \tau_B^{-1} \rangle} \tag{28b}$$

Note that if the hard-core diameter is the same as the magnetic-core diameter ($\sigma = x$), then $\mu \propto \tau_B$, and hence $\tau_{\rm eff}(0) = \langle \tau_B \rangle$. Finally, the spectrum of the relaxation function can be computed using Eq. (22).

$$K'_{\rm id}(\omega) = \frac{1}{\langle \mu \rangle} \left\langle \frac{\mu}{1 + \omega^2 \tau_B^2} \right\rangle \tag{29a}$$

$$K''_{\rm id}(\omega) = \frac{1}{\langle \mu \rangle} \left\langle \frac{\mu \omega \tau_B}{1 + \omega^2 \tau_B^2} \right\rangle \tag{29b}$$

The essential point is that in $C_D(t)$ and $\chi_D(\omega)$, the weighting of each fraction's time dependence is proportional to μ^2, while in $m_{id}(t)$ and $K_{id}(\omega)$, the weighting is proportional to μ. To illustrate the effects of this difference, results will be discussed for two bidisperse ferrofluids, each with a particle diameter ratio equal to $\sqrt[3]{10}$, so that the ratio of the Brownian rotation times is equal to 10. Taking $\sigma = x$, this means that the ratio of dipole moments is also equal to 10, and the ratio of μ^2 is equal to 100. The configurations are defined in Table 1. In configuration A, the two fractions have equal values of $p\mu^2$, where p is the number fraction. In configuration B, the two fractions have equal values of $p\mu$. Hence, $C_D(t)$ and $\chi_D(\omega)$ for configuration A should each be a superposition of two equally weighted terms, while for configuration B, this situation holds for $m_{id}(t)$ and $K_{id}(\omega)$. To help the discussion of the results, σ, μ, and τ_B in Table 1 are all given as decimal values, although they can be defined precisely as surds.

The results for configuration A show the following features. At short times, $m_{id}(t)$ is most similar to the small-particle decay [Fig. 2(a)], but this is because the effective decay time $\tau_{eff}(0) = \langle\tau_B\rangle$ is close to the small-particle Brownian time of about $0.918\langle\tau_B\rangle$ (Table 1). Only at very long times, when the remaining magnetisation is low, does τ_{eff} approach the large-particle Brownian time of about $9.18\langle\tau_B\rangle$ [Fig. 2(b)]. Hence, $K_{id}(\omega)$ is dominated by the small-particle component, and so its main features appear at high frequency [Fig. 2(c) and (d)]. $C_D(t)$ is defined so that the small-particle and large-particle fractions make equal contributions, and hence it shows features at both short times and long times. As a result, $\chi_D(\omega)$ shows clearly resolved low-frequency and high-frequency features. The initial decay time of $C_D(t)$ is $\tau_{eff}(0) \simeq 1.67\langle\tau_B\rangle$ [Eq. (25b)], and then it switches over to the large-particle Brownian time.

The opposite situation occurs for configuration B (Fig. 3), since the small-particle and large-particle fractions make equal contributions to $m_{id}(t)$, but the large-particle fraction makes the dominant contribution to $C_D(t)$. As a result, $K_{id}(\omega)$ shows clearly resolved features at low frequency and high frequency, while $C_D(\omega)$ is swamped by the low-frequency band corresponding to large particles. Note that the short-time behaviours of $C_D(t)$ and $m_{id}(t)$ are very different for this configuration (Fig. 3): the initial decay time of $C_D(t)$ is $\tau_{eff}(0) \simeq 3.03\langle\tau_B\rangle$ [Eq. (25b)], while that of $m_{id}(t)$ is equal to $\langle\tau_B\rangle$, precisely.

6.2. Interactions

Within the MMF, Weiss, and MW theories, it is very simple to include the effects of polydispersity: all that needs to be done is to replace $\chi_D(\omega)$ in Eqs. (13), (14), and (15) with the appropriate polydisperse function defined in Eq. (26) [48,53,30]. The effects of interactions on $\chi(\omega)$ are a shift in features to lower frequency, and an increase in χ, with the effects being more pronounced for larger, more strongly interacting particles [30].

The inclusion of interactions into the relaxation function is considerably more complicated in the polydisperse case. At present, the theory is not yet tractable for the Weiss and MW approaches, but it is possible to make a start using the MMF theory. At the heart

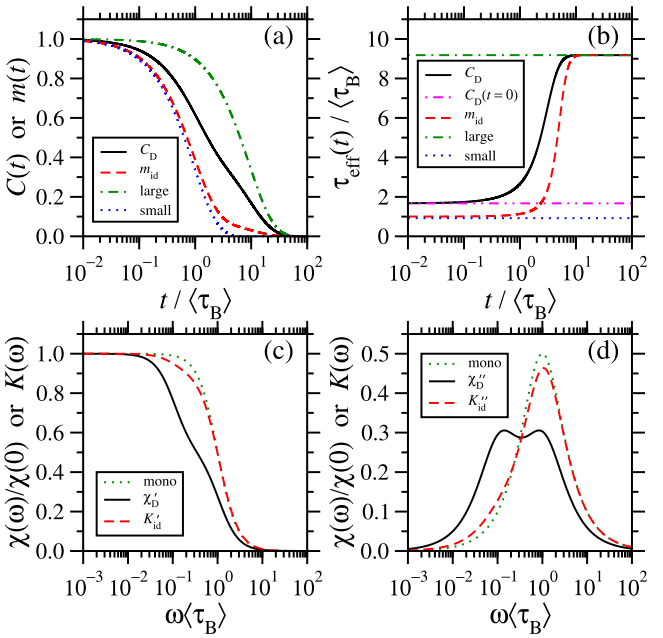

Fig. 2. Comparison between $C_D(t)$ and $m_{id}(t)$, and their spectra, for the bidisperse ferrofluid with configuration A defined in Table 1. (a) Correlation function $C_D(t)$ (solid black line), relaxation function $m_{id}(t)$ (dashed red line), and the individual-fraction relaxation functions for the large and small particles (green dot-dashed line and blue dotted line, respectively. (b) Effective relaxation time $\tau_{eff}(t)$ for $C_D(t)$ (solid black line) and $m_{id}(t)$ (red dashed line) [Eqs. (25a) and (28a), respectively]. Also shown are the Brownian rotation times for the large and small particles (green dot-dashed line and blue dotted line, respectively), and the initial decay time of $C_D(t)$ from Eq. (25b). (c) The real and (d) the imaginary parts of $\chi(\omega)$ (solid black lines) [Eq. (26)] and $K(\omega)$ (red dashed lines) [Eq. (29)]. For comparison, $\chi_D(\omega) = K_{id}(\omega)$ for a monodisperse system with $\tau_B = \langle\tau_B\rangle$ is also shown (green dotted lines).

of the approach is an equation of motion for the relaxation function $m(x_1, t)$ for each fraction [31].

$$\tau_B(x_1)\frac{dm(x_1,t)}{dt} = -m(x_1,t) + \frac{\mu_0\mu_1(x_1)M_{id}(t)}{9k_BT}\left[1 - e^{-3t/\tau_B(x_1)}\right] \quad (30)$$

Here, $M_{id}(t) = \rho\langle\mu\rangle m_{id}(t)$ is the ideal instantaneous magnetisation for the whole fluid, with $m_{id}(t)$ given by Eq. (27). (In the Weiss and MW approaches, $M_{id}(t)$ is replaced by the true instantaneous magnetisation, which has to be determined self-consistently [31].) Integrating the equation of motion gives the result

$$\begin{aligned} m(x_1,t) &= e^{-t/\tau_B(x_1)} \\ &+ \frac{\rho\mu_0\mu(x_1)e^{-t/\tau_B(x_1)}}{9k_BT}\int p(x_2)\mu(x_2)f_+(x_1,x_2)dx_2 \\ &+ \frac{\rho\mu_0\mu(x_1)e^{-t/\tau_B(x_1)}}{9k_BT}\int p(x_2)\mu(x_2)f_-(x_1,x_2)dx_2 \end{aligned} \quad (31)$$

where the functions f_+ and f_- are defined as follows.

$$f_+(x_1,x_2) = \frac{\tau_+(x_1,x_2)}{\tau_B(x_1)}\left[e^{-t/\tau_+(x_1,x_2)} - 1\right] \quad (32a)$$

$$f_-(x_1,x_2) = \frac{\tau_-(x_1,x_2)}{\tau_B(x_1)}\left[e^{t/\tau_-(x_1,x_2)} - 1\right] \quad (32b)$$

Table 1
Details of bidisperse ferrofluids with diameter ratio equal to $\sqrt[3]{10}$. p is the number fraction, σ is the particle diameter, μ is the magnetic dipole moment, and τ_B is the Brownian rotation time. The dimensionless quantities are defined such that $\langle\sigma^3\rangle = 1, \langle\mu^2\rangle = 1$, and $\langle\tau_B\rangle = 1$. In configuration A, the fractions have equal values of $p\mu^2$. In configuration B, the fractions have equal values of $p\mu$. Abbreviations: conf. is configuration; frac. is fraction.

conf.	frac.	p	σ	μ	τ_B
A	small	$\frac{100}{101}$	0.971948	0.710634	0.918182
A	large	$\frac{1}{101}$	2.093998	7.106335	9.181818
B	small	$\frac{10}{11}$	0.819321	0.316228	0.55
B	large	$\frac{1}{11}$	1.765174	3.162278	5.50

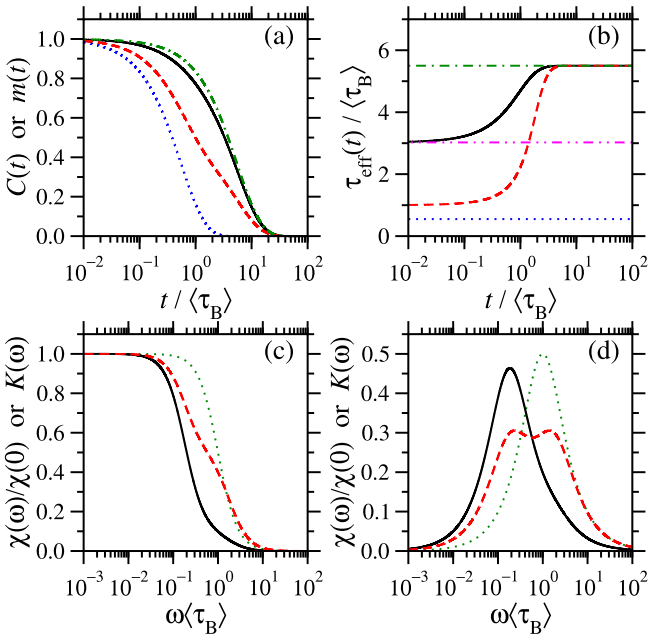

Fig. 3. Comparison between $C_{\rm D}(t)$ and $m_{\rm id}(t)$, and their spectra, for the bidisperse ferrofluid with configuration B defined in Table 1. The graphs and lines are the same as in Fig. 2.

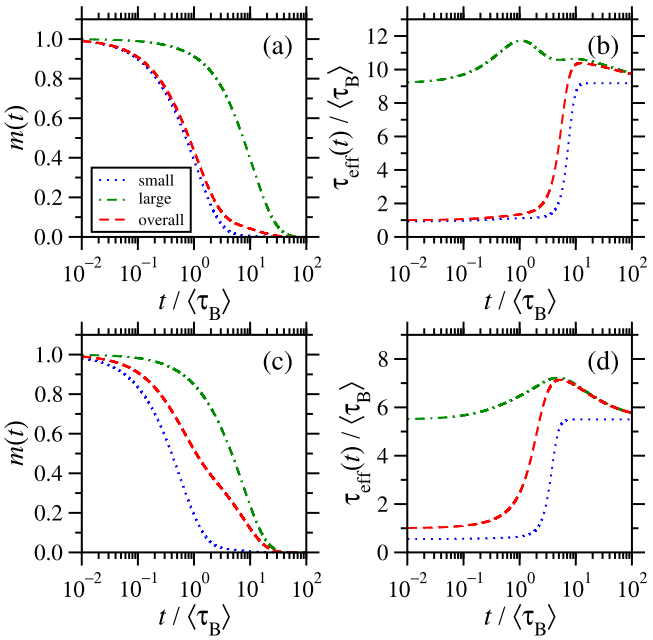

Fig. 4. Relaxation functions [(a) and (c)] and effective relaxation times [(b) and (d)] for bidisperse ferrofluids with configuration A [(a) and (b)] and configuration B [(c) and (d)] defined in Table 1, computed using the MMF approximation with an overall Langevin susceptibility $\chi_{\rm L}=1$. The dashed red lines show the results for the overall relaxation function $m_{\rm MMF}(t)$, while the green dot-dashed and blue dotted lines show the individual-fraction relaxation functions for the large and small particles, respectively.

The associated decay times are

$$\tau_{+}(x_1,x_2)=\frac{\tau_{\rm B}(x_1)\tau_{\rm B}(x_2)}{2\tau_{\rm B}(x_2)+\tau_{\rm B}(x_1)} \tag{33a}$$

$$\tau_{-}(x_1,x_2)=\frac{\tau_{\rm B}(x_1)\tau_{\rm B}(x_2)}{\tau_{\rm B}(x_2)-\tau_{\rm B}(x_1)} \tag{33b}$$

which mean that special care has to be taken with Eq. (32b); noting that $\lim_{a\to\infty}a[\exp(t/a)-1]=t, f_{-}$ reduces to $t/\tau_{\rm B}(x_1)$ when $x_1=x_2$. In the end, the total relaxation function is

$$m(t)=\frac{1}{\langle\mu\rangle}\int p(x_1)\mu(x_1)m(x_1,t)dx_1. \tag{34}$$

Clearly, the situation is quite complicated, but some illustrative results are shown for the bidisperse ferrofluids defined in Table 1. Fig. 4 shows the relaxation functions $m(t)$ and the effective relaxation times $\tau_{\rm eff}$ for each fraction and for the whole fluid, for both configurations A and B. On the one hand, the relaxation functions [Fig. 4(a) and (c)] are not very different from those shown in Figs. 2 and 3: in configuration A, the total relaxation function is dominated by the small particles; and in configuration B, the total relaxation function is an equal mix of the small-particle and large-particle functions. On the other hand, the effective relaxation times [Fig. 4 (b) and (d)] show a remarkable phenomenon: at long times, both the small-particle and total effective relaxation times converge onto the large-particle relaxation time. The presence of two local maxima in $\tau_{\rm eff}$ is a mathematical artefact of the MMF approach, as mentioned in Section 4.

The overall picture is the following. At short times, the total effective relaxation time is precisely equal to $\langle\tau_{\rm B}\rangle$, as already shown in the monodisperse and ideal polydisperse cases [note also that the second term on the right-hand side of Eq. (30), which includes the effects of interactions, is zero at $t=0$]. At long times, the small-particle magnetisation has decayed more than the large-particle magnetisation, so that the total magnetisation [$M_{\rm id}(t)$ in Eq. (30)] is dominated by the large particles; hence, the low remaining small-particle magnetisation is slaved to the large-particle magnetisation by the interactions. As a result, both the small-particle and total effective relaxation times approach the large-particle relaxation time. The situation is basically the same for both configurations A and B, with the differences arising from the weightings of each fraction.

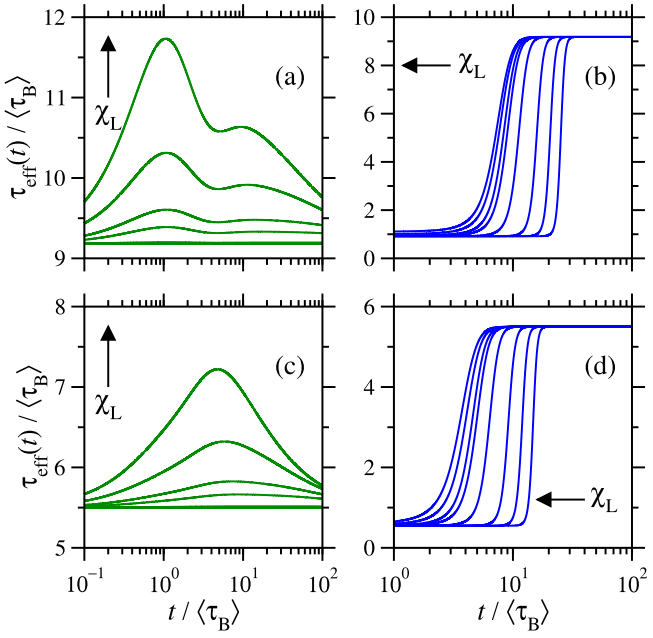

Fig. 5. Effective relaxation times for large particles [(a) and (c)] and small particles [(b) and (d)] in bidisperse ferrofluids with configuration A [(a) and (b)] and configuration B [(c) and (d)] defined in Table 1, computed using the MMF approximation with overall Langevin susceptibility $\chi_{\rm L}=1\times10^{-8},1\times10^{-6},1\times10^{-4},1\times10^{-2},0.1,0.2,0.5$, and 1. The progression of curves with increasing $\chi_{\rm L}$ is indicated by an arrow in each panel.

The effects of interaction strength are illustrated in Fig. 5, with individual large-particle and small-particle effective relaxation times with $1 \times 10^{-8} \leqslant \chi_{\mathrm{L}} \leqslant 1$, and for configurations A and B. For the large particles, the short-time and long-time relaxation times approach the corresponding Brownian time (see Table 1). Note that the MMF theory misses the fact that, at long times, the relaxation time should depend on the value of χ_{L}; this is remedied in the Weiss and MW theories, but as noted above, these are not straightforward in the polydisperse case. At intermediate times, the relaxation time increases with increasing χ_{L} due to the effects of interactions. In configuration A, the two-peaked structure is an artefact of the MMF approximation, as noted in Section 4 [31]. For the small particles, the relaxation time crosses over from the small-particle to the large-particle Brownian time, but the crossover is delayed longer with decreasing χ_{L}. Essentially, with decreasing χ_{L}, it takes longer for the second term on the right-hand side of Eq. (30) to dominate the first term.

7. Conclusions

The theoretical description of the dynamic magnetic susceptibility $\chi(\omega)$ and the magnetic relaxation $m(t)$ in monodisperse and polydisperse ferrofluids has been summarised, with a particular emphasis on the difference between equilibrium and non-equilibrium relaxation, and the effects of interactions, structure formation, and polydispersity, in the case of Brownian dynamics. In the case of monodisperse ferrofluids, it has been demonstrated that, in the presence of interactions, there are differences between $\chi(\omega)$ and the spectrum of $m(t)$, arising from the fact that the initial decay of $m(t)$ is always equal to the Brownian relaxation time, independent of interactions. In the case of polydisperse ferrofluids, including the effects of interactions is technically quite difficult. Nonetheless, using the modified mean-field theory, it is possible to show that interactions cause the small (fast) particles to relax asymptotically at a rate dictated by the large (slow) particles, which dominate the instantaneous magnetisation to which the small particles are coupled. Future work will focus on the technical question of how to incorporate better descriptions of the interactions, such as in the Weiss and modified-Weiss theories.

Regarding the relevance to experiments, it should be possible to use the theories outlined here to fit functions to the measured susceptibility or relaxation function and determine the particle-size distribution – so-called dynamic magnetogranulometry [62,63]. On the basis of the current work, the best choice of method depends on the sample, and the relative contributions of the different particle fractions to the averages of $\langle\mu\rangle$ and $\langle\mu^2\rangle$. If the contributions of differently sized particles to $\langle\mu^2\rangle$ are comparable, then the dynamic magnetic susceptibility would give the best resolution of particle sizes. Note that this condition also means that each fraction has roughly the same Langevin susceptibility, although the presence of interactions leads to differences between the true static susceptibilities. If the contributions of differently sized particles to $\langle\mu\rangle$ are comparable, then magnetic relaxation would give the best resolution of particle sizes.

CRediT authorship contribution statement

Alexey O. Ivanov: Conceptualisation, Calculation, Writing. **Philip J. Camp:** Conceptualisation, Calculation, Writing, Reviewing and Editing.

Declaration of Competing Interest

The authors declare that they have no known competing financial interests or personal relationships that could have appeared to influence the work reported in this paper.

Acknowledgements

A.O.I. gratefully acknowledges research funding from the Ministry of Science and Higher Education of the Russian Federation (Ural Federal University project within the Priority 2030 Program).

References

[1] R.E. Rosensweig, Ferrohydrodynamics, Dover Publications Inc, New York, 1998.
[2] S.H. Chung, A. Hoffmann, S.D. Bader, C. Liu, B. Kay, L. Makowski, L. Chen, Biological sensors based on Brownian relaxation of magnetic nanoparticles, Appl. Phys. Lett. 85 (2004) 2971–2973.
[3] C. Barrera, V. Florián-Algarin, A. Acevedoa, C. Rinaldi, Monitoring gelation using magnetic nanoparticles, Soft Matter 6 (2010) 3662–3668.
[4] V.L. Calero Diaz del Castillo, D.I. Santiago-Quiñonez, C. Rinaldi, Quantitative nanoscale viscosity measurements using magnetic nanoparticles and SQUID ac susceptibility measurements, Soft Matter 7 (2011) 4497–4503.
[5] R.S.M. Rikken, R.J.M. Nolte, J.C. Maan, J.C.M. van Hest, D.A. Wilson, P.C.M. Christianen, Manipulation of micro- and nanostructure motion with magnetic fields, Soft Matter 10 (2014) 1295–1308.
[6] Q.A. Pankhurst, J. Connolly, S.K. Jones, J. Dobson, Applications of magnetic nanoparticles in biomedicine, J. Phys. D: Appl. Phys. 36 (2003) R167–R181.
[7] Q.A. Pankhurst, N.T.K. Thanh, S.K. Jones, J. Dobson, Progress in applications of magnetic nanoparticles in biomedicine, J. Phys. D: Appl. Phys. 42 (2009) 224001.
[8] R. Hergt, R. Hiergeist, I. Hilger, W. Kaiser, Y. Lapatnikov, S. Margel, U. Richter, Maghemite nanoparticles with very high ac-losses for application in RF-magnetic hyperthermia, J. Magn. Magn. Mater. 270 (2004) 345–357.
[9] F. Sonvico, S. Mornet, S. Vasseur, C. Dubernet, D. Jaillard, J. Degrouard, J. Hoebeke, E. Duguet, P. Colombo, P. Couvreur, Folate-conjugated iron oxide nanoparticles for solid tumor targeting as potential specific magnetic hyperthermia mediators: Synthesis, physicochemical characterization, and in vitro experiments, Bioconjug. Chem. 16 (2005) 1181–1188.
[10] J.-P. Fortin, C. Wilhelm, J. Servais, C. Ménager, J.-C. Bacri, F. Gazeau, Size-sorted anionic iron oxide nanomagnets as colloidal mediators for magnetic hyperthermia, J. Am. Chem. Soc. 129 (2007) 2628–2635.
[11] R.E. Rosensweig, Heating magnetic fluid with alternating magnetic field, J. Mag. Magn. Mater. 252 (2002) 370–374.
[12] R. Müller, R. Hergt, M. Zeisberger, W. Gawalek, Preparation of magnetic nanoparticles with large specific loss power for heating applications, J. Mag. Magn. Mater. 289 (2005) 13–16.
[13] Yu.L. Raikher, V.I. Stepanov, Physical aspects of magnetic hyperthermia: Low-frequency ac field absorption in a magnetic colloid, J. Mag. Magn. Mater. 368 (2014) 421–427.
[14] M. Boskovic, G.F. Goya, S. Vranjes-Djuric, N. Jovic, B. Jancar, B. Antic, Influence of size distribution and field amplitude on specific loss power, J. Appl. Phys. 117 (2015) 103903.
[15] A.F. Pshenichnikov, A.V. Lebedev, Dynamic susceptibility of magnetic liquids, Sov. Phys. JETP 68 (1989) 498–502.
[16] B.H. Erné, K. Butter, B.W.M. Kuipers, G.J. Vroege, Rotational diffusion in iron ferrofluids, Langmuir 19 (2003) 8218–8225.
[17] F. Ludwig, A. Guillaume, M. Schilling, N. Frickel, A.M. Schmidt, Determination of core and hydrodynamic size distributions of $CoFe_2O_4$ nanoparticle suspensions using ac susceptibility measurements, J. Appl. Phys. 108 (2010) 033918.
[18] R.M. Ferguson, A.P. Khandhar, C. Jonasson, J. Blomgren, C. Johansson, K.M. Krishnan, Size-dependent relaxation properties of monodisperse magnetite nanoparticles measured over seven decades of frequency by ac susceptometry, IEEE Trans. Magn. 49 (2013) 3441–3444.
[19] D. Eberbeck, S. Hartwig, U. Steinhoff, L. Trahms, Description of the magnetisation decay in ferrofluids with a narrow particle size distribution, Magnetohydrodynamics 39 (2003) 77.
[20] F. Ludwig, S. Mäuselein, E. Heim, M. Schilling, Magnetorelaxometry of magnetic nanoparticles in magnetically unshielded environment utilizing a differential fluxgate arrangement, Rev. Sci. Instrum. 76 (2005) 106102.
[21] D. Eberbeck, F. Wiekhorst, U. Steinhoff, L. Trahms, Aggregation behaviour of magnetic nanoparticle suspensions investigated by magnetorelaxometry, J. Phys.: Condens. Matter 18 (2006) S2829–S2846.
[22] F. Ludwig, E. Heim, D. Menzel, M. Schilling, Investigation of superparamagnetic Fe_3O_4 nanoparticles by fluxgate magnetorelaxometry for use in magnetic relaxation immunoassays, J. Appl. Phys. 99 (2006) 08P106.
[23] F. Ludwig, E. Heim, M. Schilling, Characterization of superparamagnetic nanoparticles by analyzing the magnetization and relaxation dynamics using fluxgate magnetometers, J. Appl. Phys. 101 (2007) 113909.
[24] J. Dieckhoff, D. Eberbeck, M. Schilling, F. Ludwig, Magnetic-field dependence of Brownian and Néel relaxation times, J. Appl. Phys. 119 (2016) 043903.

[25] J. Fock, C. Balceris, R. Costo, L. Zeng, F. Ludwig, M.F. Hansen, Field-dependent dynamic responses from dilute magnetic nanoparticle dispersions, Nanoscale 10 (2018) 2052–2066.
[26] P. Lemal, S. Balog, L. Ackermann-Hirschi, P. Taladriz-Blanco, A.M. Hirt, B. Rothen-Rutishauser, M. Lattuada, A. Petri-Fink, Simple and fast evaluation of relaxation parameters of magnetic nanoparticles, J. Mag. Mag. Mater. 499 (2020) 166176.
[27] W.F. Brown Jr., Thermal fluctuations of a single-domain particle, J. Appl. Phys. 34 (1963) 1319–1320.
[28] W.F. Brown Jr., Thermal fluctuations of a single-domain particle, Phys. Rev. 130 (1963) 1677–1686.
[29] W.F. Brown Jr., Thermal fluctuation of fine ferromagnetic particles, IEEE Trans. Magn. 15 (1979) 1196–1208.
[30] A.O. Ivanov, P.J. Camp, Theory of the dynamic magnetic susceptibility of ferrofluids, Phys. Rev. E 98 (2018) 050602(R).
[31] A.O. Ivanov, P.J. Camp, Effects of interactions on magnetization relaxation dynamics in ferrofluids, Phys. Rev. E 102 (2020) 032610.
[32] H. Fröhlich, Theory of dielectrics: dielectric constant and dielectric loss, 2nd Edition., Clarendon Press, Oxford, 1987.
[33] J.-P. Hansen, I.R. McDonald, Theory of Simple Liquids, 3rd Edition., Academic Press, London, 2006.
[34] J.O. Sindt, P.J. Camp, S.S. Kantorovich, E.A. Elfimova, A.O. Ivanov, Influence of dipolar interactions on the magnetic susceptibility spectra of ferrofluids, Phys. Rev. E 93 (2016) 063117.
[35] T.M. Batrudinov, Yu.E. Nekhoroshkova, E.I. Paramonov, V.S. Zverev, E.A. Elfimova, A.O. Ivanov, P.J. Camp, Dynamic magnetic response of a ferrofluid in a static uniform magnetic field, Phys. Rev. E 98 (2018) 052602.
[36] P.J. Camp, A.O. Ivanov, J.O. Sindt, How chains and rings affect the dynamic magnetic susceptibility of a highly clustered ferrofluid, Phys. Rev. E 103 (2021) 062611.
[37] P. Debye, Polar Molecules, Chemical Catalog Company, New York, 1929.
[38] A.Yu. Zubarev, A.V. Yushkov, Dynamic properties of moderately concentrated magnetic liquids, J. Exp. Theor. Phys. 87 (1998) 484–493.
[39] B.U. Felderhof, R.B. Jones, Mean field theory of the nonlinear response of an interacting dipolar system with rotational diffusion to an oscillating field, J. Phys.: Condens.Matter 15 (2003) 4011–4024.
[40] P. Ilg, S. Hess, Nonequilibrium dynamics and magnetoviscosity of moderately concentrated magnetic liquids: A dynamic mean-field study, Z. Naturforsch. 58 (2003) 589–600.
[41] P.M. Déjardin, F. Ladieu, Nonlinear susceptibilities of interacting polar molecules in the self-consistent field approximation, J. Chem. Phys. 140 (2014) 034506.
[42] A. Fang, Generic theory of the dynamic magnetic response of ferrofluids, Soft Matter 16 (2020) 10928–10934.
[43] A. Fang, Dynamical effective field model for interacting ferrofluids: I. Derivations for homogeneous, inhomogeneous, and polydisperse cases, J. Phys.: Condens. Matter 34 (2022) 115102.
[44] A. Fang, Dynamical effective field model for interacting ferrofluids: II. The proper relaxation time and effects of dynamic correlations, J. Phys.: Condens. Matter 34 (2022) 115103.
[45] E.L. Verde, G.T. Landi, J.A. Gomes, M.H. Sousa, A.F. Bakuzis, Magnetic hyperthermia investigation of cobalt ferrite nanoparticles: Comparison between experiment, linear response theory, and dynamic hysteresis simulations, J. Appl. Phys. 111 (2012) 123902.
[46] M.A. Martens, R.J. Deissler, Y. Wu, L. Bauer, Z. Yao, R. Brown, M. Griswold, Modeling the Brownian relaxation of nanoparticle ferrofluids: Comparison with experiment, Med. Phys. 40 (2013) 022303.
[47] G.T. Landi, Role of dipolar interaction in magnetic hyperthermia, Phys. Rev. B 89 (2014) 014403.
[48] A.O. Ivanov, V.S. Zverev, S.S. Kantorovich, Revealing the signature of dipolar interactions in dynamic spectra of polydisperse magnetic nanoparticles, Soft Matter 12 (2016) 3507–3513.
[49] A.O. Ivanov, S.S. Kantorovich, V.S. Zverev, E.A. Elfimova, A.V. Lebedev, A.F. Pshenichnikov, Temperature-dependent dynamic correlations in suspensions of magnetic nanoparticles in a broad range of concentrations: a combined experimental and theoretical study, Phys. Chem. Chem. Phys. 18 (2016) 18342–18352.
[50] Yu.A. Buyevich, A.O. Ivanov, Equilibrium properties of ferrocolloids, Phys. A 190 (1992) 276–294.
[51] A.F. Pshenichnikov, V.V. Mekhonoshin, A.V. Lebedev, Magneto-granulometric analysis of concentrated ferrocolloids, J. Mag. Magn. Mater. 161 (1996) 94–102.
[52] A.O. Ivanov, O.B. Kuznetsova, Magnetic properties of dense ferrofluids: An influence of interparticle correlations, Phys. Rev. E 64 (2001) 041405.
[53] A.O. Ivanov, S.S. Kantorovich, V.S. Zverev, A.V. Lebedev, A.F. Pshenichnikov, P.J. Camp, Concentration-dependent zero-field magnetic dynamic response of polydisperse ferrofluids, J. Mag. Magn. Mater. 459 (2018) 252–255.
[54] A.O. Ivanov, S.S. Kantorovich, E.A. Elfimova, V.S. Zverev, J.O. Sindt, P.J. Camp, The influence of interparticle correlations and self-assembly on the dynamic initial magnetic susceptibility spectra of ferrofluids, J. Mag. Magn. Mater. 431 (2017) 141–144.
[55] D.V. Berkov, N.L. Gorn, R. Schmitz, D. Stock, Langevin dynamic simulations of fast remagnetization processes in ferrofluids with internal magnetic degrees of freedom, J. Phys.: Condens. 18 (Matter 2006,) S2595–S2621.
[56] D.V. Berkov, L.Yu. Iskakova, A.Yu. Zubarev, Theoretical study of the magnetization dynamics of nondilute ferrofluids, Phys. Rev. E 79 (2009) 021407.
[57] P.M. Déjardin, Magnetic relaxation of a system of superparamagnetic particles weakly coupled by dipole-dipole interactions, J. Appl. Phys. 110 (2011) 113921.
[58] P. Ilg, M. Kröger, Dynamics of interacting magnetic nanoparticles: effective behavior from competition between Brownian and Néel relaxation, Phys. Chem. Chem. Phys. 22 (2020) 22244–22259.
[59] M. Klokkenburg, R.P.A. Dullens, W.K. Kegel, B.H. Erné, A.P. Philipse, Quantitative real-space analysis of self-assembled structures of magnetic dipolar colloids, Phys. Rev. Lett. 96 (2006) 037203.
[60] L. Rovigatti, J. Russo, F. Sciortino, Structural properties of the dipolar hard-sphere fluid at low temperatures and densities, Soft Matter 8 (2012) 6310–6319.
[61] S. Kantorovich, A.O. Ivanov, L. Rovigatti, J.M. Tavares, F. Sciortino, Nonmonotonic magnetic susceptibility of dipolar hard-spheres at low temperature and density, Phys. Rev. Lett. 110 (2013) 148306.
[62] A.O. Ivanov, O.B. Kuznetsova, P.J. Camp, Dynamic magnetogranulometry of ferrofluids, J. Mag. Magn. Mater. 498 (2020) 166153.
[63] A.O. Ivanov, V.S. Zverev, Dynamic susceptibility of ferrofluids: The numerical algorithm for the inverse problem of magnetic granulometry, Mathematics 9 (2021) 2450.